Characterization and Functional Evaluation of Surface Texture of Micro Eccentric Shaft Based on Multi-index

Minghui Cheng
Beijing Institute of Technology
Li Jiao
Beijing Institute of Technology
Pei Yan (pyan@bit.edu.cn)
Beijing Institute of Technology
Zhongke Niu
Aerospace System Engineering Shanghai
Tianyang Qiu
Beijing Institute of Technology
Xibin Wang
Beijing Institute of Technology
Baorong Zhang
Shanxi Diesel Engine Industry Co

Research Article

Keywords: Micro eccentric shaft, Deformation compensation, Surface texture characterization, Functional evaluation, Turn-milling

Posted Date: March 18th, 2021

DOI: https://doi.org/10.21203/rs.3.rs-304920/v1

Version of Record: A version of this preprint was published at Proceedings of the Institution of Mechanical Engineers, Part B: Journal of Engineering Manufacture on February 25th, 2022. See the published version at https://doi.org/10.1177/09544054221078078.

Characterization and Functional Evaluation of Surface Texture of Micro Eccentric Shaft Based on Multi-index

Minghui Cheng[a], Li Jiao[a], Pei Yan[a*], Zhongke Niu[b], Tianyang Qiu[a], Xibin Wang[a], Baorong Zhang[c]

[a] *Key Laboratory of Fundamental Science for Advanced Machining, Beijing Institute of Technology, Beijing100081, China.*
[b] *Aerospace System Engineering Shanghai, Shanghai 201108, China.*
[c] *Shanxi Diesel Engine Industry Co., Ltd, Shanxi 037000, China.*
**Corresponding author: Tel: +86-10-6891-2716, Email: pyan@bit.edu.cn.*

Abstract

Micro eccentric shaft has important application in many high-tech fields because of its small specific gravity, material and energy saving. The surface texture generated during processing has an indispensable influence on the surface integrity and the final functional capability. However, due to the micro scale and weak rigidity, it is difficult to characterize the surface texture and evaluate the functionality by traditional quantitative parameters. In order to comprehensively realize the surface texture characterization and functional analysis, a mathematical model is established to analyze the surface texture machined with different cutting tools. The machining deformation of the micro eccentric shaft machined during turn-milling with different cutting tools is compensated. Then the surface microscopic profile and functional performance of the surface texture are analyzed by amplitude distribution function (ADF) and bearing area curve (BAC), and the surface texture is also evaluated by fractal dimension, which can avoid the effect of scale and resolution. Furthermore, power spectrum density (PSD) is utilized to analyze the relationship between the process dynamic state and geometrical specification of the surface texture. It is shown that the microscopic height distribution of surface machined by flat end milling cutter tends to be more random and there are more microscopic geometric features than that of the ball end milling cutter. The machined surface obtained by the flat end milling cutter has better load bearing, wear resistance and

liquid retention capability.

Keywords: Micro eccentric shaft, Deformation compensation, Surface texture characterization, Functional evaluation, Turn-milling.

1 Introduction

Micro eccentric shaft can realize the transformation of rotary motion and linear motion, which is widely used in micro machinery. Because of the eccentric characteristic of micro eccentric shaft, the process of machining is very complex, and the machining precision is difficult to guarantee. Turn-milling is suitable for machining micro eccentric shaft, because the radial force during machining is small [1] and the vibration characteristics are greatly improved, compared to turning [2]. However, due to the small scale of micro eccentric shaft, it is difficult to meet the requirements of evaluation length of the traditional surface profile characterization parameters, which makes it difficult to accurately characterize the actual surface quality of micro eccentric shaft.

Characterization of surface texture is an important aspect in the surface quality evaluation of parts. Modeling and simulation of the machined surface have become the research focus to characterize surface texture in recent years. Theoretically, surface topography simulation can be achieved by studying the tool's motion trajectory and the residual height left on the machined surface. Yuan et al. developed a geometrical surface roughness model to analyze the influence degree of cutting parameters [3]. Karagüzel et al. studied the form errors of machined surface including circularity, cusp height and circumferential surface roughness from the perspective of cutting mechanism [4]. Zhu et al. built the mathematical model to describe theoretical surface topography according to the establishment of locus function [5]. Similarly, Döbberthin et al. established a function of surface micro height with respect to cutting parameters and realized the simulation of surface topography obtained by using flat end milling

cutter [6]. Overall, simulation of surface texture machined by different cutting tools has been achieved in orthogonal turn-milling. However, most of the research focuses on the modeling of surface texture from the perspective of the machined surface shape, which has a relatively large error compared to the actual machined surface. What's more, few studies have further analyzed the specific microscopic geometrical feature and functional performance of surface texture in orthogonal turn-milling process.

Generally speaking, the evaluation of surface texture includes two aspects. One is to evaluate the surface micro geometric features through some quantitative indicators and the other is to select reasonable parameters to evaluate the functional properties of the machined surface [7]. The quantitative characterization parameters not only include commonly used two-dimensional (2D) amplitude parameters such as arithmetical mean height R_a and root mean square height R_q, but also include the three-dimensional (3D) amplitude parameters, spatial parameters and functional parameters [8, 9]. Therefore, it is insufficient to characterize the surface texture just using the 2D amplitude parameters. 3D amplitude and functional parameters are needed to characterize the surface texture and perform functional analysis. Eifler et al. realized the performance verification of areal surface texture based on the S_k-parameters associated with functional characteristic [10]. Shi et al. proposed an evaluation method for 3D surface roughness based on sampling array to evaluate surface quality [11]. In addition, some statistical functions have been developed to describe the machined surface in other engineering field. For example, amplitude distribution function is the commonly used to describe the probability distribution of surface micro height and characterize the geometrical features [12, 13], and bearing area curve as a statistical function has a superior performance in assessing the wear resistance, load bearing, and lubricant or oil retention capacity of the machined surface [14, 15]. Furthermore, 3D amplitude and functional parameters belong to time-dominant quantification parameters, which cannot explain the

dynamic frequency information of the machined surface. Therefore, some statistical functions such as power spectrum density and continuous wavelet transform have been used to analyze the spectral characteristic of microscopic profile [16, 17]. Through the above parameters or statistical functions, the characterization and functional analysis of the machined surface can be fully realized. However, the machined surface obtained by orthogonal turn-milling is often characterized by 2D amplitude parameters [18-21]. It is inadequate for comprehensively describing the machined surface, especially for the micro parts.

In this paper, a mathematical model is firstly established to analyze the difference of surface texture under different cutting tools. Then, due to the weak stiffness of the micro eccentric shaft in machining, the deformation of the micro eccentric shaft is compensated. The amplitude distribution function and bearing area curve are used to analyze the functional performance of the machined surface and the fractal dimension is used to analyze the surface texture, which can avoid the influence of scale and resolution compared with traditional quantitative statistical parameters. Finally, the spectral performance of surface texture is analyzed by combining power spectral density function with continuous wavelet transform. The characterization and functional performance of the surface texture obtained by different cutting tools are realized.

2 Theoretical analysis and experimental setup

2.1 The mathematical model of surface texture

In order to analyze the difference of machined surface and study the microscopic surface topography characteristics, the mathematical model of surface texture is first established according to theoretical model of cutting edge trajectory [22, 23]. Figure 1 shows the geometric mathematical model of orthogonal turn-milling cylinder by ball end milling cutter. It is assumed that the workpiece does not move and the tool

rotates relative to the workpiece when constructing the model. Taking the ball end milling cutter as an example, the calculation process of the model is as follows:

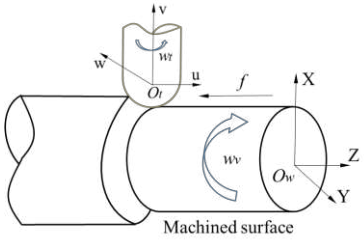

Figure 1: The mathematical model for machined surface by ball end milling cutter

The coordinates of any point on the helical edge of the ball end milling cutter under the tool coordinate system O_t-uvw are shown in Eq.1:

$$\begin{cases} u = R_t \sin\alpha \cos\left[\tan\gamma \ln(\cot\alpha/2)\right] \\ w = R_t \sin\alpha \sin\left[\tan\gamma \ln(\cot\alpha/2)\right] \\ v = -R_t \cos\alpha \end{cases} \tag{1}$$

Where R_t is the cutting tool radius, α is the position angle of spiral edge, and γ is the helix angle of the ball end milling cutter.

During the cutting process of the tool, the angle between the *i*-th blade and the *u*-axis at any time can be represented as Eq.2, so the coordinate value (*U, W, V*) of any point on each helical edge is shown in Eq.3:

$$\varphi_i = \varphi_0 + 2\pi(i-1)/m - w_t t \tag{2}$$

$$\begin{Bmatrix} U \\ W \\ V \end{Bmatrix} = \begin{bmatrix} \cos\varphi_i & -\sin\varphi_i & 0 \\ \sin\varphi_i & \cos\varphi_i & 0 \\ 0 & 0 & 1 \end{bmatrix} \begin{Bmatrix} u \\ w \\ v \end{Bmatrix} \tag{3}$$

Where w_t is cutting tool angular velocity, and $w_t t$ represents the angle that the cutting has turned at the current time *t*.

In the next step, the transformation matrix is used to make the coordinate axes of the workpiece coordinate system O_w-XYZ corresponding to that of the tool coordinate system O_t-uvw . The transformation matrix is shown in Eq.4:

$$T=\begin{bmatrix} 0 & \sin(\omega_w t) & \cos(\omega_w t) & 0 \\ 0 & -\cos(\omega_w t) & \sin(\omega_w t) & 0 \\ 1 & 0 & 0 & 0 \\ 0 & 0 & 0 & 1 \end{bmatrix} \tag{4}$$

The coordinate origin of tool coordinate system O_t-uvw in the coordinate system O_w-XYZ is expressed as Eq.5:

$$\begin{cases} x_0 = R_t + R_w - a_p \\ y_0 = 0 \\ z_0 = f \cdot t \end{cases} \tag{5}$$

Where f represents the tool axial feed, R_w represents the radius of workpiece, and a_p represents the cutting depth.

When considering the kinematic error of machine spindle, the transformation matrix of ball end milling cutter center in the O_w-XYZ coordinate system can be expressed as Eq.6:

$$T_Q=\begin{bmatrix} 1 & 0 & 0 & f \cdot t + \Delta d_1 \cdot \dfrac{\cos(\Delta\alpha_1 + \varphi_0 - \omega_t)}{2} \\ 0 & 1 & 0 & \dfrac{\Delta d_1}{2} \cdot \sin(\Delta\alpha_1 + \varphi_0 - \omega_t) \\ 0 & 0 & 1 & R_t + R_w - a_p + \dfrac{\Delta d_2}{2} \cdot \sin(\Delta\alpha_2 + \varphi_0 - \omega_t) \\ 0 & 0 & 0 & 1 \end{bmatrix} \tag{6}$$

Where Δd_1 is the radius of the rotating spindle, and Δd_2 is axial drift amplitude. Finally, the coordinates of any point on the ball end milling cutter edge in the workpiece coordinate system O_w-XYZ can be derived as follows:

$$\begin{bmatrix} x \\ y \\ z \\ 1 \end{bmatrix} = T \cdot T_Q \cdot T_y \cdot \begin{bmatrix} U \\ W \\ V \\ 1 \end{bmatrix} \tag{7}$$

On this basis, the cylindrical workpiece was meshed along the axial and circumferential direction. In order to simulate the surface texture, the machined surface, the cutting edge of the tool and the machining time need to be discretized. The coordinate points of the cutting edge in the workpiece coordinate system were compared with the corresponding coordinate points of the machined surface at

different time to determine whether the tool has cut into the workpiece. Then the residual height on the workpiece surface was calculated. Finally, the 3D surface texture can be obtained according to the residual height of the machined surface. The flowchart of the simulation process is shown in Figure 2.

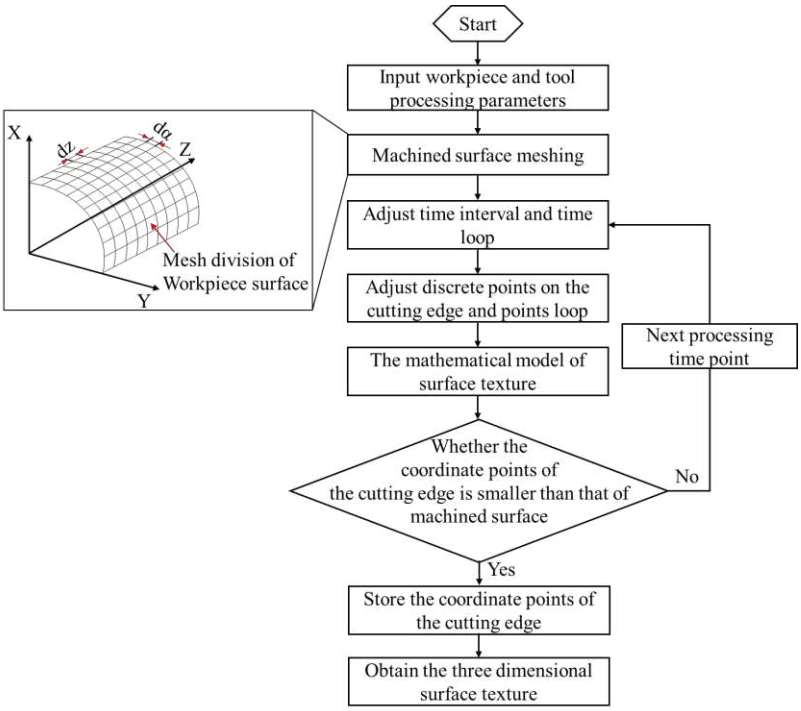

Figure 2: Flowchart of the simulation process

2.2 Machining deformation compensation

Due to the weak rigidity of micro eccentric shaft, large deformation easily occurs during orthogonal turn-milling, which has a great influence on the machining precision. In this paper, the expression of machining deformation is given, and the expression of variable cutting depth is studied to compensate the machining deformation.

The machining process of micro shaft is usually simplified as a cantilever beam model, as shown in Figure 3.

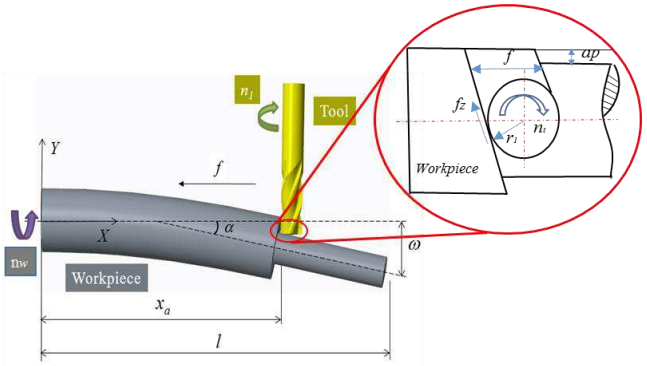

Figure 3: Simplified model of the machining process of micro shaft

Where n_t is the rotational speed of tool, r_1 is the radius of tool, n_w is the rotational speed of workpiece, a_p is the depth of cut, f is the axial feed rate, and f_z is the circumferential feed rate.

According to the mechanics characteristic of the material, the deformation of the cutting point is given by:

$$\omega(x) = \frac{F(x)x^3}{3EI} \tag{8}$$

Where $F(x)$ is the cutting force, E is the modulus of elasticity and I is the polar moment of inertia.

The value of machining deformation varies with the position of the workpiece. So in this paper a method is proposed to improve the machining deformation by varying the depth of cut. The relation between the actual depth of cut and the designed depth of cut is given by:

$$a_p'(x) - \omega'(x) = a_p \tag{9}$$

Where $a_p'(x)$ is the actual depth of cut, $\omega'(x)$ is the actual machining deformation and $a_p(x)$ is the designed depth of cut. Substituting equation 9 to equation 10:

$$a_p'(x) - \frac{F'(x)x^3}{3EI} = a_p \tag{10}$$

The cutting force is proportional to the depth of cut:

$$F'(x) = ka_p'(x) \tag{11}$$

Where k is the ratio coefficient. Substituting equation 11 to equation 10:

$$a_p'(x) = \frac{3EIa_p}{3EI - kx^3} \tag{12}$$

Finally, the expression of the variable depth of cut $a_p'(x)$ is obtained.

2.3 Statistical analysis functions

Normally, specific machining process corresponds to a certain surface with specific microscopic geometrical feature and functional performance. What's more, when the value of surface roughness is greater than 0.1μm, the evaluation length should be greater than 4 mm to ensure the validity of the result. Because the size of micro eccentric shaft is difficult to meet the requirement of the evaluation length as shown in Figure 5, it is insufficient to characterize the surface texture just with traditional quantitative parameters. So other functional statistical parameters are needed to characterize the surface texture and perform functional analysis. Amplitude distribution function is the commonly used to describe the probability distribution of surface micro height and characterize the geometrical features. In addition, the bearing area curve has a superior performance in assessing the wear resistance, load-bearing, and lubricant or oil retention capacity of the machined surface. The original surface profile and corresponding functional statistical parameters are shown in Figure 4 and Table 1, respectively.

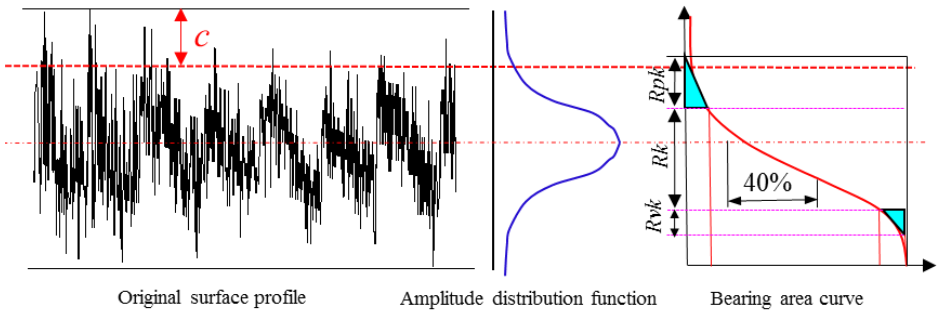

Figure 4: The 2D surface profile and corresponding ADF and BAC

Table 1: The description of BAC-related functional statistical parameters

	BAC-related parameters	Description
R_{pk}	Reduced peak height	The average height of peak section above the core roughness profile
R_k	Core height	The difference of heights between the material ratio values from 0% and 100% on the equivalent line
R_{vk}	Reduced dale height	The average height of dale section below the core roughness profile

In addition, considering the fractal dimension is an independent parameter for scale, which not be

influenced by the sampling length, box fractal dimension is introduced in this paper to evaluate the surface quality [24， 25]. Furthermore, the machined surface includes a lot of dynamic frequency information during the machining process, such as the trajectory of the tool path and machine vibration, but the time-dominant quantification parameters are lack of the quantitative spectrum analysis. Therefore, power spectrum density and continuous wavelet transform are combined to analyze the spectral characteristic of microscopic profile in this research.

2.4 Experimental setup

The micro eccentric shaft with eccentricity of 0.15 mm is machined as shown in Figure 5. The material of the workpiece is 310S stainless steel and the properties are shown in Table 2.

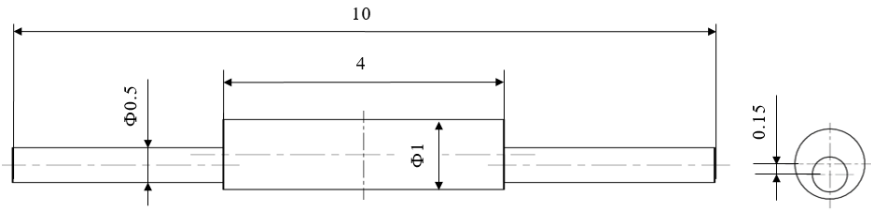

Figure 5: The size information of the micro eccentric shaft

Table 2: Main physical properties of 310S stainless steel

Density	Elastic Modulus	Poisson ratio	Yield strength	Tensile strength	Brinell Hardness
7.98g/cm^3	195GPa	0.29	⩾205MPa	⩾520MPa	187

The cutting tools used in the paper are shown in **Error! Not a valid bookmark self-reference.** and the corresponding cutting parameters are shown in Table 3.

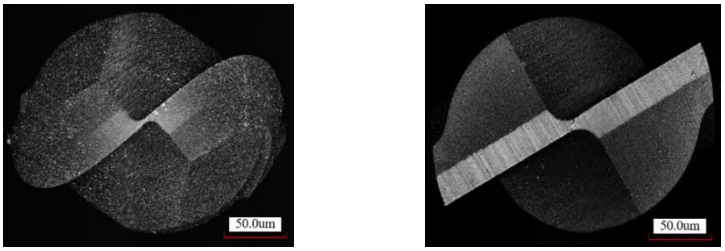

(a) Micro ball end milling cutter (b) Micro flat end milling cutter

Figure 6: The micro milling cutter

Table 3: Specific parameters of micro milling cutter

Cutting tool materials	Cutting tool diameter(mm)	Cutting edge number	Helix angle(°)
WC-TiC-Co cemented carbide	0.2	2	55

CNC turn-milling machining center KNC-50FS is used to machine the micro eccentric shaft. KEYENCE VK-100 microscope is used for measuring the machined surface texture. The turn-milling and measuring process is shown in Figure 7, and corresponding deformation compensation cutting parameters and actual cutting parameters are listed in Table 4 and Table 5, respectively.

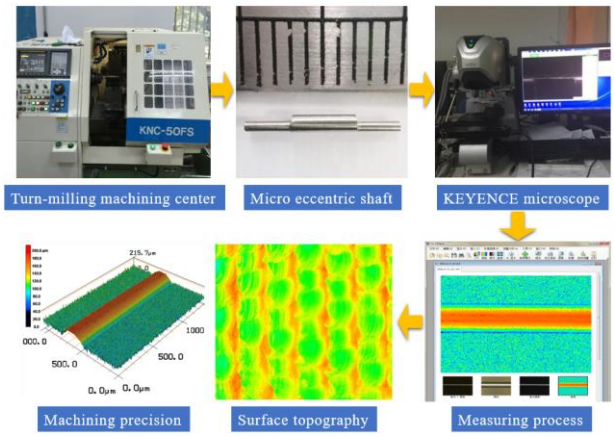

Figure 7: Turn-milling and measuring process

Table 4: Experimental parameters for the machining deformation compensation model

Clamp	Rotation speed of cutting tool (r/min)	Rotation speed of workpiece (r/min)	Depth of cut (mm)	Axial feed rate (mm/r)
1	4500	30	0.1	0.02
2	5500	30	0.1	0.02

Table 5: Experimental parameters to explore the machined surface texture

Number	Rotation speed of cutting tool (r/min)	Rotation speed of workpiece (r/min)	Depth of cut (mm)	Axial feed rate (mm/r)
1	4000,4500,5000,5500	30	0.05	0.02
2	4500	25,30,35,40	0.05	0.02
3	4500	30	0.04,0.05,0.06,	0.02
4	4500	30	0.05	0.018,0.02,0.022,

3 Results and discussion

3.1 Compensation analysis of machining deformation

Due to the low stiffness of the micro eccentric shaft, the resistance to elastic deformation is poor.

Under the influence of cutting force, it is easy to produce large deflection deformation, and the machining accuracy is reduced. So the machining deformation should be compensated.

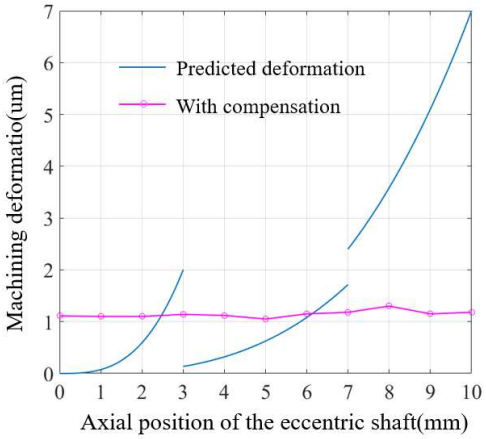

Figure 8: The machining deformation of micro eccentric shaft

The deformation of the eccentric shaft after machining deformation compensation is shown in Figure 8. The predicted machining deformation of micro eccentric shaft increases sharply with the increase of the axial position, and the largest value 7 μm is located at the end of the micro eccentric shaft. Since the micro eccentric shaft was divided into three stages during machining, there were three stages of deformation as shown in Figure.8. When the axial position of the eccentric shaft is 3 mm and 7 mm, in accordance with the principle of controlling a larger amount of deformation, the greater of the two machining deformation value is taken. Benefited from the machining precision control model, the machining deformation reduces to 1 μm, which means that the machining precision increased 86%.

3.2 Surface texture characterization and functional performance analysis

After machining deformation compensation, two different types of micro-milling cutters are used in the milling experiment under the same cutting parameters, then the machined surface texture is captured by the KEYENCE microscope. At a rotation speed of cutting tool of 4000 r/mm, a rotation speed of workpiece of 30 r/mm, a depth of cut of 0.05 mm, a axial feed rate of 0.02 mm/r, the simulation

results and experimental results of surface texture profile with different cutting tools are shown in Figure 9. The simulation results have a relatively high degree of consistency with the experimental results. The surface texture obtained by the flat end milling cutter is arranged in wavy stripes, and there are many sharp peaks formed on the surface. The surface texture obtained by the ball end milling cutter is arranged in a spiral shape (ring-shape pit) and many small peaks appear on the edge of ring-shape pit. Therefore, it is significant to analyze the functional performance of different surface texture and dynamic characteristics under different machining conditions.

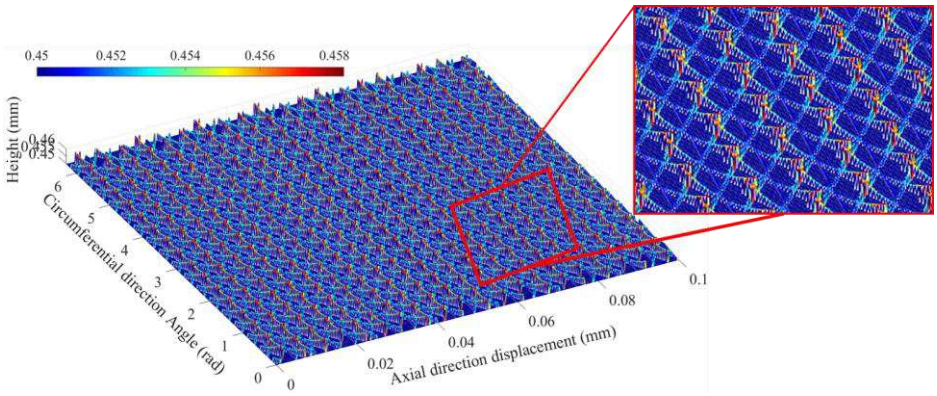

(a) The simulation results of surface texture of flat end milling cutter

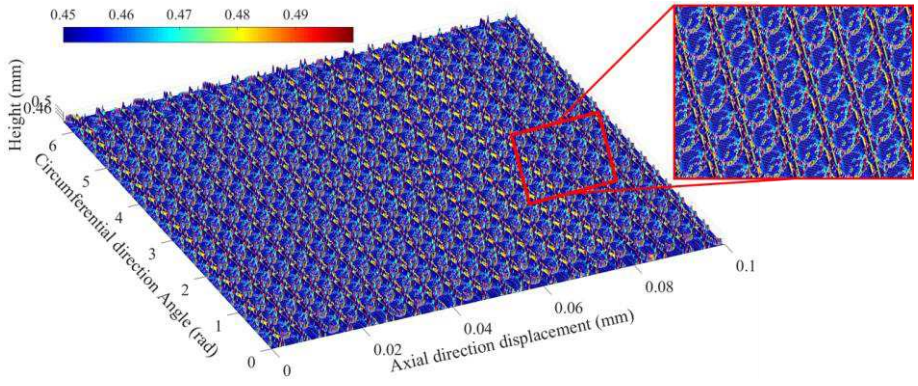

(b) The simulation results of surface texture of ball end milling cutter

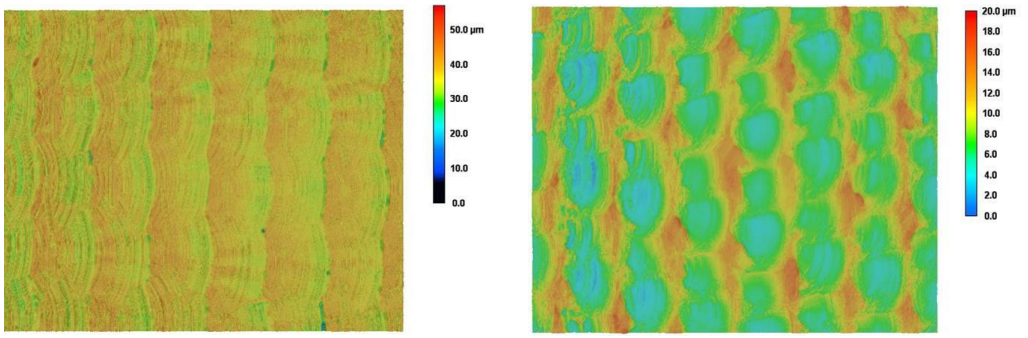

(c) Experimental results of flat end milling cutter (d) Experimental results of ball end milling cutter

Figure 9: Surface texture profiles with different cutting tools.

Firstly, there is a clear difference in the height of the surface microscopic profile. The amplitude distribution function (ADF) is used to analyze the probabilistic density of the surface profile height. The analysis results of different cutting tools under intermediate level combination of cutting parameters are shown in Figure 10, and the statistical parameters of the ADF under all cutting parameter combinations are shown in Figure 11.

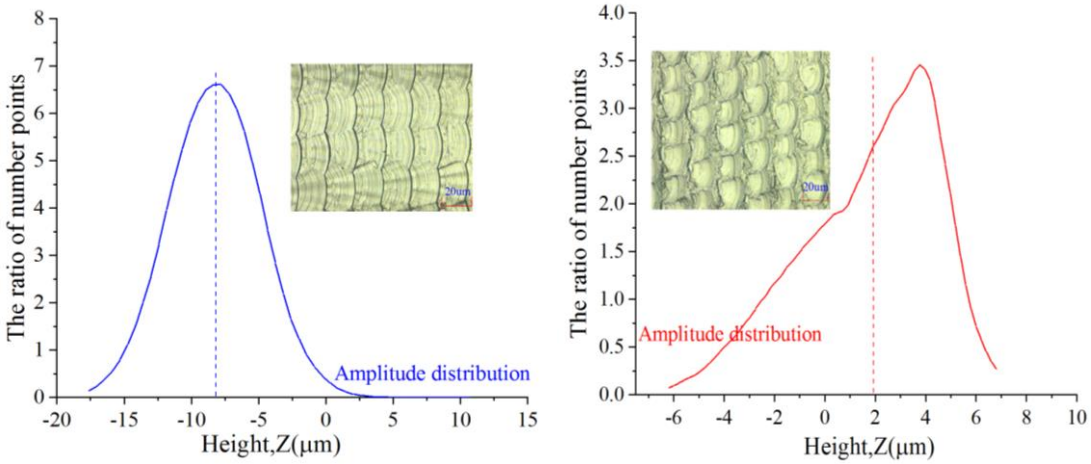

(a) The ADF of flat end milling cutter (b) The ADF of ball end milling cutter

Figure 10: ADFs under different cutting tools

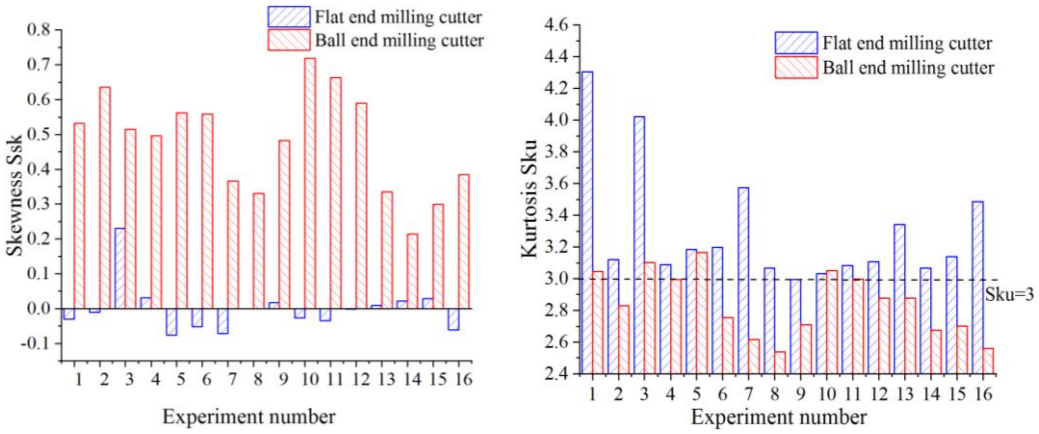

(a) The values of Skewness (b) The values of Kurtosis

Figure 11: Statistical parameters of the machined surface

As shown in Figure 10 and Figure 11(a), when machining with flat end milling cutter, the skewness values of the surface are approximately zero, which means that the microscopic height distribution of the surface is much closer to Gaussian distribution and the surface texture tends to be more random (more micro geometrical features). The ADF of the surface machined by the ball end milling cutter are positively deviated from Gaussian distribution, which indicates that the surface height region above the mean line has a higher probability density. In addition, the leptokurtic surface has a high S_{ku} value (> 3), while the platykurtic surface has a low S_{ku} value (< 3). It can be inferred from Figure 11(b), there are more sharp peaks on the surface machined by flat end milling cutter, which corresponds to the previous research [3] and the simulation results as shown in Figure 9(a).

Conventional surface texture evaluation parameters are rarely associated with functionality-related performance. It is necessary to propose functional statistical parameters to characterize the corresponding functionality-related performance of machined surface. In general, the microscopic height of the surface texture corresponds to different performance of the part. Therefore, the functional performance of the surface texture is evaluated with the bearing area curve (BAC), as shown in Figure 12.

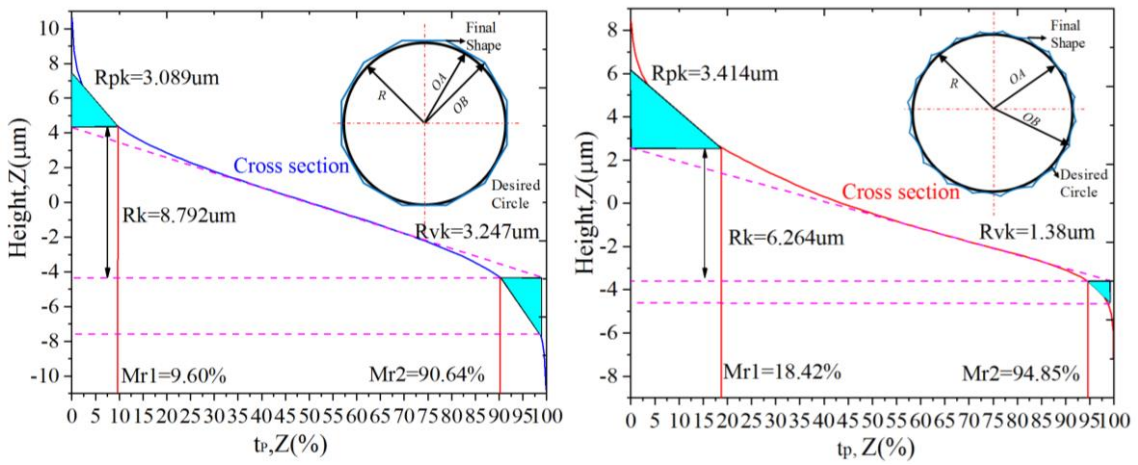

(a) The BAC of flat end milling cutter (b) The BAC of ball end milling cutter

Figure 12: BAC under different cutting tools

Figure 12 shows the functional statistical parameters under different cutting tools. Functionally, reduced peak height R_{pk} is directly related to the initial mechanical contact in the running-in period, which affects the time for the part to enter the normal working state and the actual wear amount of the material. The larger value of R_{pk} means the poor running-in performance. Core height R_k directly sustains the corresponding loads and determines the wear resistance of the machined surface. Higher value of R_k indicates the longer service life of the part. Reduced dale height R_{vk} is used to characterize the fluid retention property of the surface. Higher value of R_{vk} represents a better fluid retention capacity. Functional statistical parameters of the machined surface under all cutting parameter combinations are shown in Figure 13.

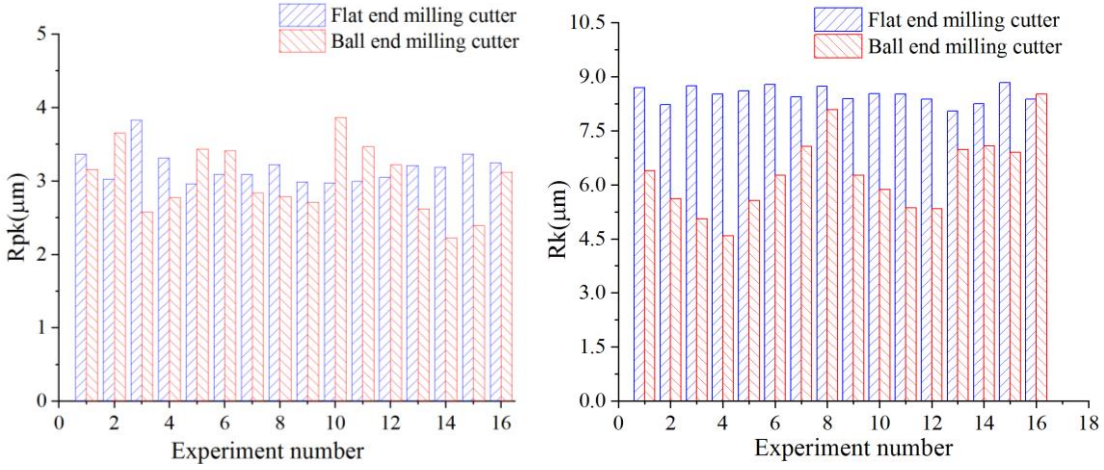

(a) The values of R_{pk} (b) The values of R_k

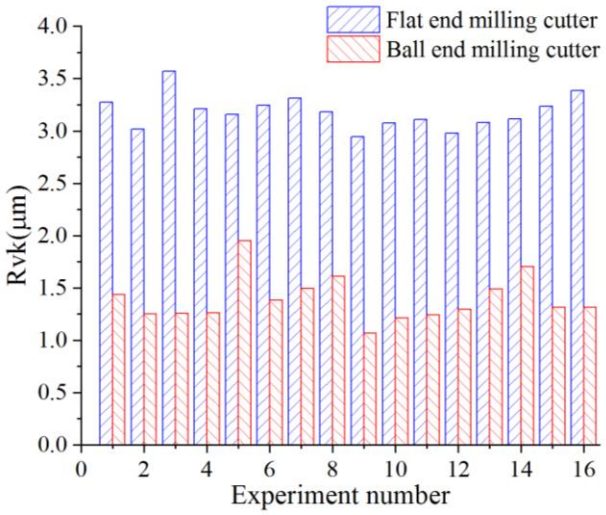

(c) The values of R_{vk}

Figure 13: Functional statistical parameters under all cutting parameter combinations

As shown in Figure 13(b) and Figure 13(c), values of R_k and R_{vk} of the surface machined by the flat end milling cutter are much larger than that of the ball end milling cutter under the same cutting parameters, which indicates that the surface machined by the flat end milling cutter has better load bearing, wear resistance and lubricant or oil retention capability. This is mainly because that the cross section of the surface machined by the flat end milling cutter is not an ideal circle but a polygonal shape, according to previous research [5], which means that the height difference of the microscopic profile varies widely. Moreover, wave-shaped peaks and valleys staggered with each other are formed on the surface, so the regular wavy cutting marks in the horizontal and vertical direction are formed on the machined surface as shown in Figure 9(a). Such a surface can form a better lubricant retention structure in sliding friction pair [26]. However, scallops are formed on the surface machined by ball end milling cutter and circular dimples exist at the bottom of valley [27] as shown in Figure 9(b), which accounts for the mediocre performance of the surface. The values of R_{pk} is slightly different as shown in Figure 13 (a), which indicates that there is no significant distinction in the running-in performance of the surface.

Considering that micro eccentric shaft belongs to micro-small parts, the surface texture is often

affected by the scale or resolution. The fractal dimension is not affected by scale and resolution, which is usually used to measure the texture feature and complexity of the surface. The surface texture is analyzed by the fractal dimension, as shown in Figure 14.

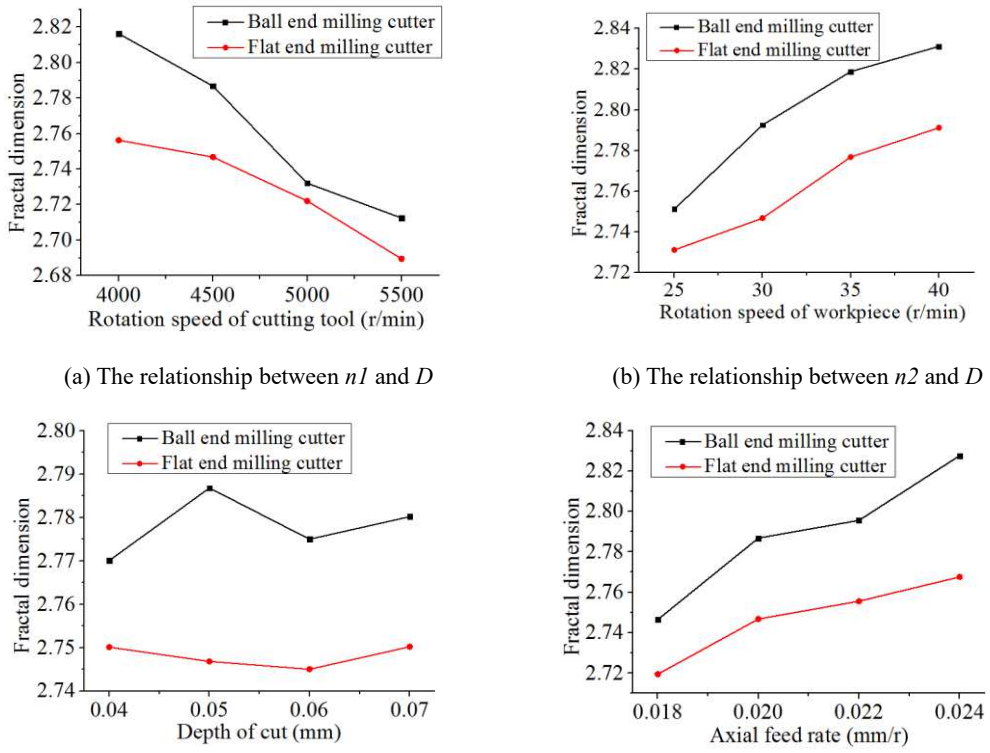

(a) The relationship between *n1* and *D*

(b) The relationship between *n2* and *D*

(c) The relationship between a_p and *D*

(d) The relationship between *f* and *D*

Figure 14: The relationship between cutting parameters and fractal dimension *D*

As shown in Figure 14, the relationship between cutting parameters and fractal dimension *D* of the surface texture with different types of the cutting tool is coincident. It can be found that the value of the fractal dimension obtained by the ball end milling cutter is slightly larger than that of the flat end milling cutter. This suggests that the micro profile obtained by the ball end milling cutter is more regularity, while the profile morphology of the flat end milling cutter is more complex, and the surface profile has overall fluctuation.

3.4 Spectral analysis of the surface texture

Traditional surface quantitative parameters can't explain the exact relations between process

dynamic state and geometrical specification of the machined surface [28], so the functional parameter PSD is introduced to study the spectral properties of the machined surface. The spectrum analysis process of surface texture is similar for each set of cutting parameters. Therefore, the cutting parameter combinations under variable axial feed rate are selected for analysis as shown in Figure 15.

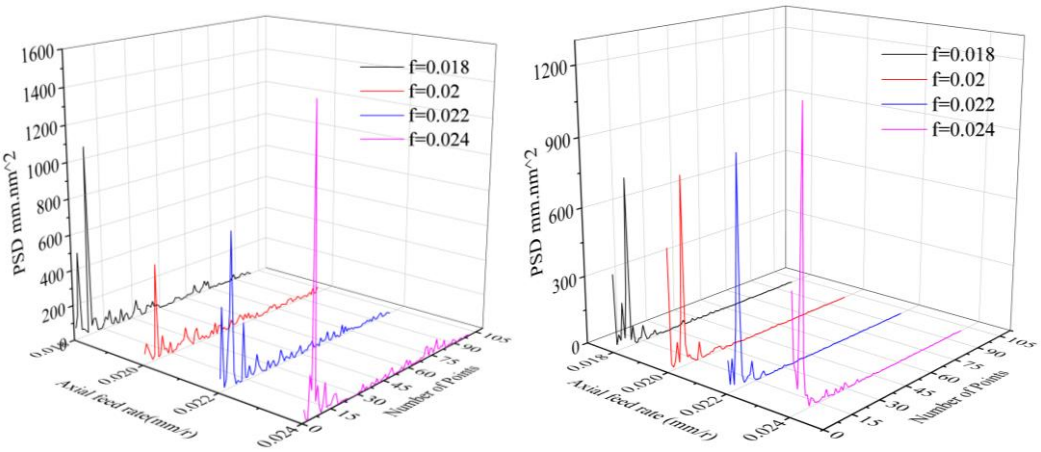

(a)PSD analysis results of flat end milling cutter (b) PSD analysis results of ball end milling cutter

Figure 15: PSD analysis results under different cutting parameters

As can be seen from Figure 15, in addition to the vicinity of the peak, the PSD curve of the surface obtained by the flat end milling cutter fluctuates in a zigzag manner, and the PSD curve of the surface obtained by the ball end milling cutter is relatively flat. It shows that the surface texture obtained by the flat end milling cutter has more micro geometrical features than that of the ball end milling cutter, which is consistent with the results of Figure 11(a) and the chatter is slightly larger in the orthogonal turn-milling process. Furthermore, both of the PSD have a dominant spatial frequency, which indicates that the surfaces have periodic microscopic structure as shown in Figure 9.

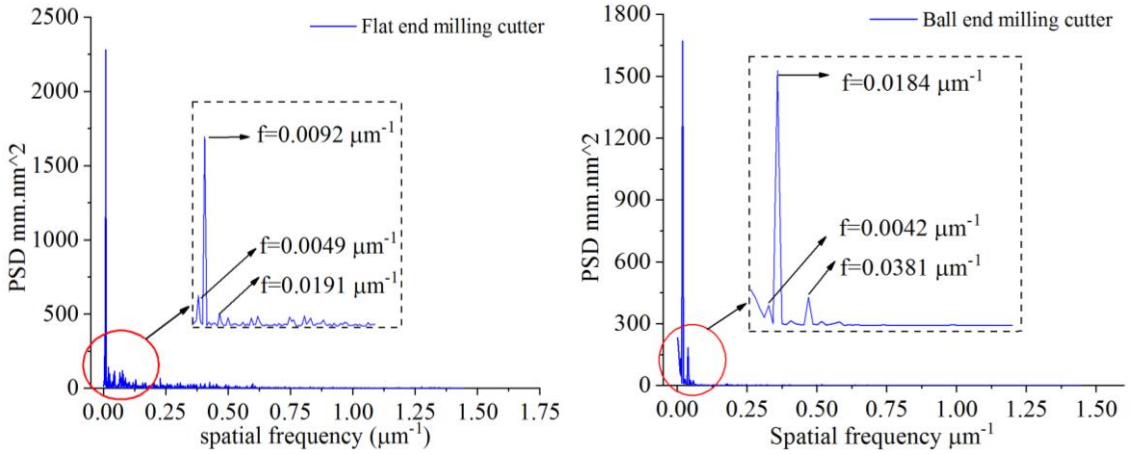

(a) PSD analysis of flat end milling cutter (b) PSD analysis of ball end milling cutter

Figure 16: PSD analysis under different cutting tools

From the results of PSD analysis, it can be seen that there are three apparent actual frequency characteristics corresponding to the surface obtained by different cutting tools as shown in Figure 16. Continuous wavelet analysis can remedy the shortcoming of PSD in analyzing the continuity of frequency features, so the wavelet coefficients are extracted from the actual frequency characteristics using continuous wavelet analysis (CWT), and the frequency components are determined. The effect of cutting parameters on the microscopic profile is mainly reflected by the wavelength and amplitude of frequency characteristics. The relation between cutting parameters and frequency characteristics can be established by obtaining the dominant frequency. Corresponding to the flat end milling cutter, the frequency characteristic of 0.0092 μm^{-1} is the main factor affecting the surface texture. Similarly, the frequency characteristic of 0.0184 μm^{-1} is the main factor affecting the surface texture for ball end milling cutter as shown in Figure 17. In addition, intermediate frequency characteristic is the most important factor to reflect the influence of cutting parameters and cutting vibration.

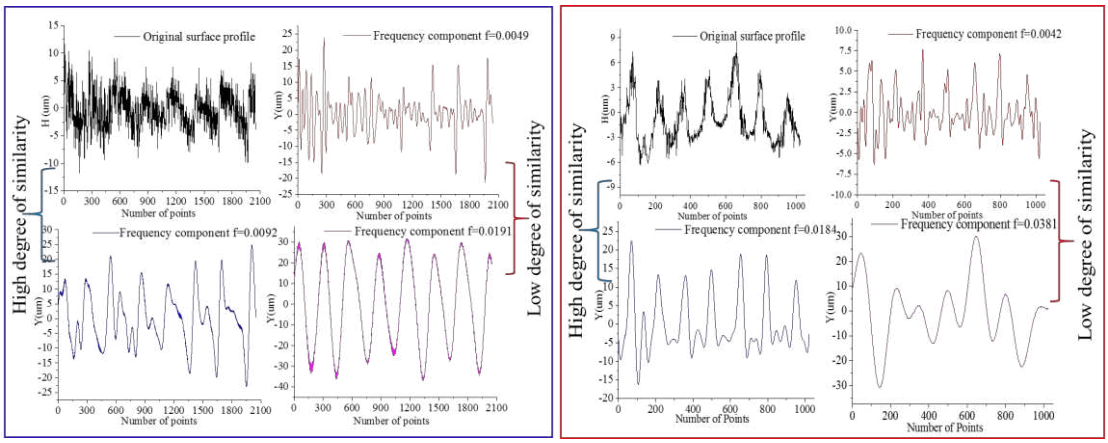

(a) CWT analysis of flat end milling cutter (b) CWT analysis of ball end milling cutter

Figure 17: Wavelet analysis results under different scale factors

4 Conclusions

Surface texture characterization plays an important part for describing surface micro geometrical features and determining surface functionality-related properties. In this paper, the surface texture obtained by different cutting tools during turn-milling of micro eccentric shaft is analyzed from the perspective of functional characterization parameters and statistical functions. The main conclusions can be summarized as follows:

(1) The machining deformation of micro eccentric shaft is calculated based on cutting forces, then the machining precision model is obtained and the machining precision increased 86% benefited from that;

(2) The microscopic height distribution of the surface machined by flat end milling cutter is much closer to Gaussian distribution, and there are more microscopic geometric features than that of the ball end milling cutter;

(3) The machined surface obtained by the flat end milling cutter has better load bearing, wear resistance and lubricant or oil retention capability compared with ball end milling cutter;

(4) The influence of cutting parameters and vibration on machined surface can be reflected by intermediate frequency characteristic during machining process.

Funding This work is supported by "National Key Research and Development Program of China (2018YFB2002202)" and "National Natural Science Foundation of China (52075040)".

Data availability Not applicable.

Compliance with ethical standards

Competing interests The authors declare that they have no competing interests.

Ethical approval Not applicable.

Consent to participate Not applicable.

Consent to publish Not applicable.

References

[1] Otalora-Ortega H, Osoro PA, Arrazola Arriola PJ. (2019) Analytical modeling of the uncut chip geometry to predict cutting forces in orthogonal centric turn-milling operations. International Journal of Machine Tools and Manufacture,144:103428. doi: 10.1016/j.ijmachtools.2019.103428

[2] Sun T, Qin L, Fu Y, Hou J. (2019) Chatter stability of orthogonal turn-milling analyzed by complete discretization method. Precision Engineering,56:87-95. doi: 10.1016/j.precisioneng.2018.10.012

[3] Yuan SM, Zheng WW. (2011) The Surface Roughness Modeling on Turn-Milling Process and Analysis of Influencing Factors. Applied Mechanics and Materials,117-119:1614-1620. doi: 10.4028/www.scientific.net/AMM.117-119.1614

[4] Karagüzel U, Uysal E, Budak E, Bakkal M. (2015) Analytical modeling of turn-milling process geometry, kinematics and mechanics. International Journal of Machine Tools and Manufacture,91:24-33. doi: 10.1016/j.ijmachtools.2014.11.014

[5] Zhu L, Li H, Wang W. (2013) Research on rotary surface topography by orthogonal turn-milling. The International Journal of Advanced Manufacturing Technology,69:2279-2292. doi: 10.1007/s00170-013-5202-8

[6] Döbberthin C, Taschenberger S, Welzel F, Woschke E. (2019) Modelling of turn-milled surfaces. The International Journal of Advanced Manufacturing Technology,101:849-857. doi: 10.1007/s00170-018-2921-x

[7] De Chiffre L, Lonardo P, Trumpold H, Lucca DA, Goch G, Brown CA, Raja J, et al. (2000) Quantitative Characterisation of Surface Texture. CIRP Annals - Manufacturing Technology,49:635, 642-644, 652. doi: 10.1016/S0007-8506(07)63458-1

[8] Gadelmawla ES, Koura MM, Maksoud TMA, Elewa IM, Soliman HH. (2002) Roughness parameters. Journal of materials processing technology,123:133-145. doi: 10.1016/S0924-0136(02)00060-2

[9] Liang X, Liu Z, Yao G, Wang B, Ren X. (2019) Investigation of surface topography and its deterioration resulting from tool wear evolution when dry turning of titanium alloy Ti-6Al-4V. Tribology International,135:130-142. doi: 10.1016/j.triboint.2019.02.049

[10] Eifler M, Klauer K, Kirsch B, Aurich JC, Seewig J. (2021) Performance verification of areal surface texture measuring instruments with the Sk-parameters. Measurement,173:108550. doi: 10.1016/j.measurement.2020.108550

[11] Shi H, Yuan S, Li Z, Song H, Qian J. (2019) Evaluation of surface roughness based on sampling array for rotary ultrasonic machining of carbon fiber reinforced polymer composites. Measurement,138:175-181. doi: 10.1016/j.measurement.2019.02.002

[12] Yang D, Liu Z. (2015) Surface topography analysis and cutting parameters optimization for peripheral milling titanium alloy Ti − 6Al − 4V. International Journal of Refractory Metals and Hard Materials,51:192-200. doi: 10.1016/j.ijrmhm.2015.04.001

[13] Zeng Q, Qin Y, Chang W, Luo X. (2018) Correlating and evaluating the functionality-related properties with surface texture parameters and specific characteristics of machined components. International Journal of Mechanical Sciences,149:62-72. doi: 10.1016/j.ijmecsci.2018.09.044

[14] Dong WP, Sullivan PJ, Stout KJ. (1992) Comprehensive study of parameters for characterizing three-dimensional surface topography I: Some inherent properties of parameter variation. Wear,159:161-171. doi: https://doi.org/10.1016/0043-1648(92)90299-N

[15] Dong WP, Sullivan PJ, Stout KJ. (1993) Comprehensive study of parameters for characterizing three-dimensional surface topography II: Statistical properties of parameter variation. Wear,167:9-21. doi: https://doi.org/10.1016/0043-1648(93)90050-V

[16] Cheung CF, Lee WB. (2001) Characterisation of nanosurface generation in single-point diamond turning. International journal of machine tools & manufacture,41:851-875. doi: 10.1016/S0890-6955(00)00102-4

[17] Zahouani H, Mezghani S, Vargiolu R, Dursapt M. (2008) Identification of manufacturing signature by 2D wavelet decomposition. Wear,264:480-485. doi: 10.1016/j.wear.2006.08.047

[18] Boozarpoor M, Teimouri R, Yazdani K. (2021) Comprehensive study on effect of orthogonal turn-milling parameters on surface integrity of Inconel 718 considering production rate as constrain. International Journal of Lightweight Materials and Manufacture,4:145-155. doi: 10.1016/j.ijlmm.2020.09.002

[19] Choudhury SK, Bajpai JB. (2005) Investigation in orthogonal turn-milling towards better surface finish. Journal of Materials Processing Technology,170:487-493. doi: 10.1016/j.jmatprotec.2004.12.010

[20] Choudhury SK, Mangrulkar KS. (2000) Investigation of orthogonal turn-milling for the machining of rotationally symmetrical work pieces. Journal of materials processing technology,99:120-128. doi: 10.1016/S0924-0136(99)00397-0

[21] Jin CZ, Fang R. (2014) Research on Surface Topography and Roughness of Micro Parts by High Speed Turn-Milling. Materials Science Forum,800-801:607-612. doi: 10.4028/www.scientific.net/MSF.800-801.607

[22] Hu HCJ. (2018) Research on Surface Micro Pattern Generation in Turn-Milling Considering Ball-End Milling Cutter Eccentricity. Advances in Engineering Research,149:855-863. doi:

[23] Peng Z, Jiao L, Yan P, Yuan M, Gao S, Yi J, Wang X. (2018) Simulation and experimental study on 3D surface topography in micro-ball-end milling. The International Journal of Advanced Manufacturing Technology,96:1943-1958. doi: 10.1007/s00170-018-1597-6

[24] Li J, Du Q, Sun C. (2009) An improved box-counting method for image fractal dimension estimation. Pattern Recognition,42:2460-2469. doi: 10.1016/j.patcog.2009.03.001
[25] Niu Z, Jiao L, Chen S, Yan P, Wang X. (2018) Surface Quality Evaluation in Orthogonal Turn-Milling Based on Box-Counting Method for Image Fractal Dimension Estimation. Nanomanufacturing and Metrology,1:125-130. doi: 10.1007/s41871-018-0015-x
[26] Zhu L, Jiang Z, Shi J, Jin C. (2015) An overview of turn-milling technology. The International Journal of Advanced Manufacturing Technology,81:493-505. doi: 10.1007/s00170-015-7187-y
[27] Kaibu S, Ikeda A, Ihara Y. (2018) Study on Cutting Marks by Turn Mill Process. Procedia CIRP,77:251-254. doi: 10.1016/j.procir.2018.09.008
[28] Nieslony P, Krolczyk GM, Wojciechowski S, Chudy R, Zak K, Maruda RW. (2018) Surface quality and topographic inspection of variable compliance part after precise turning. Applied Surface Science,434:91-101. doi: 10.1016/j.apsusc.2017.10.158

Table captions

Figure captions

Figures

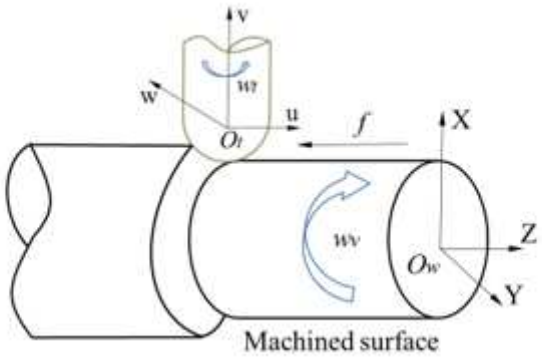

Figure 1

The mathematical model for machined surface by ball end milling cutter

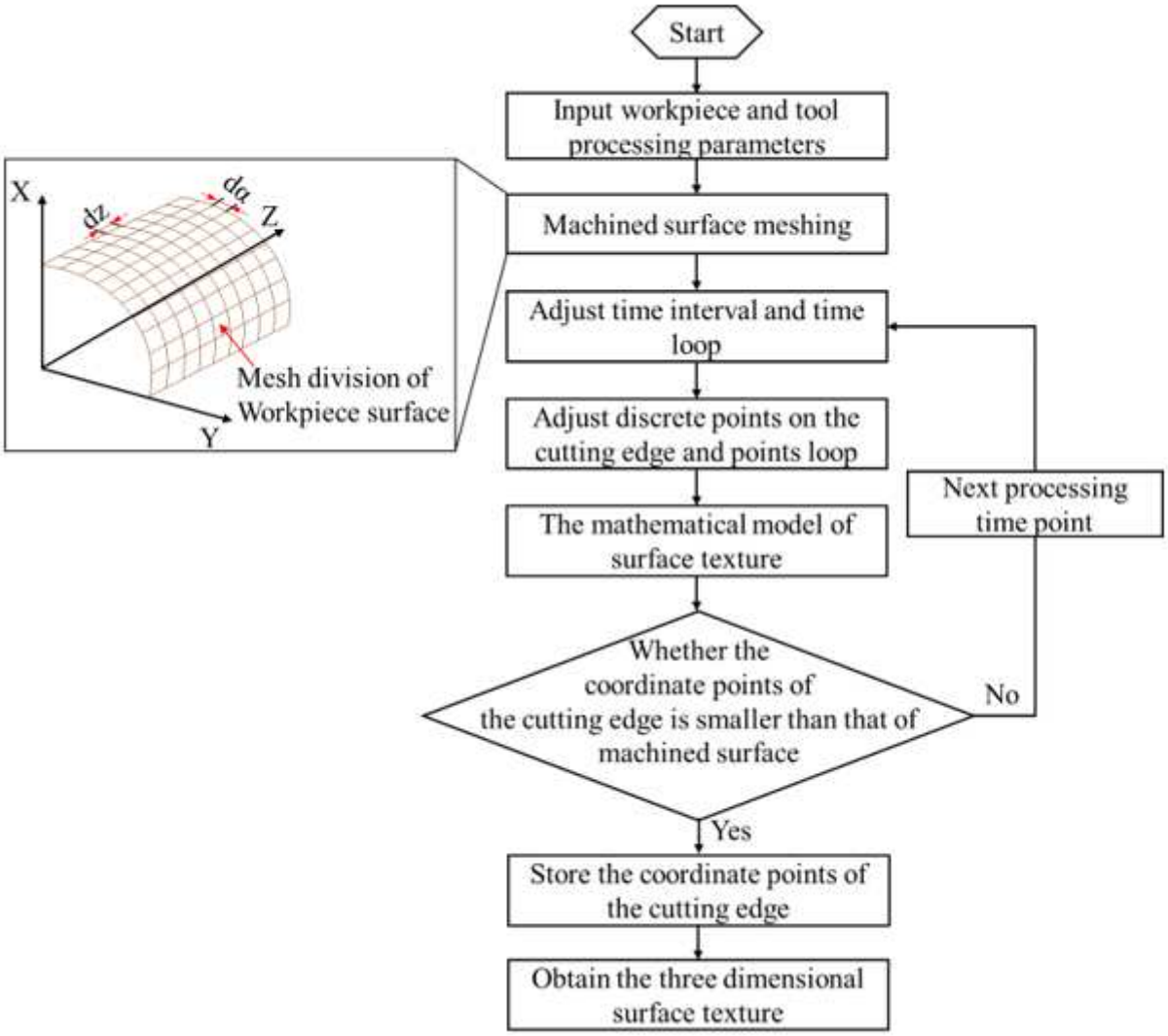

Figure 2

Flowchart of the simulation process

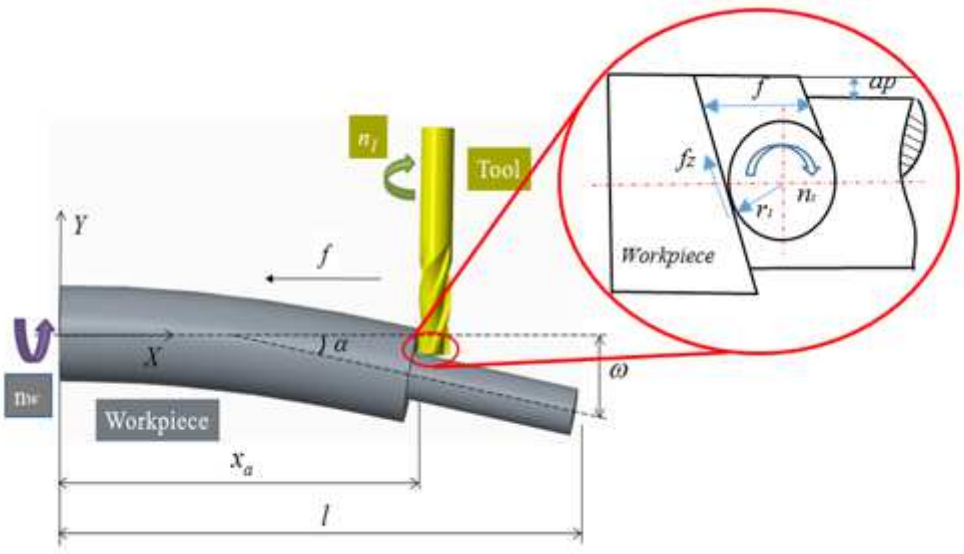

Figure 3

Simplified model of the machining process of micro shaft

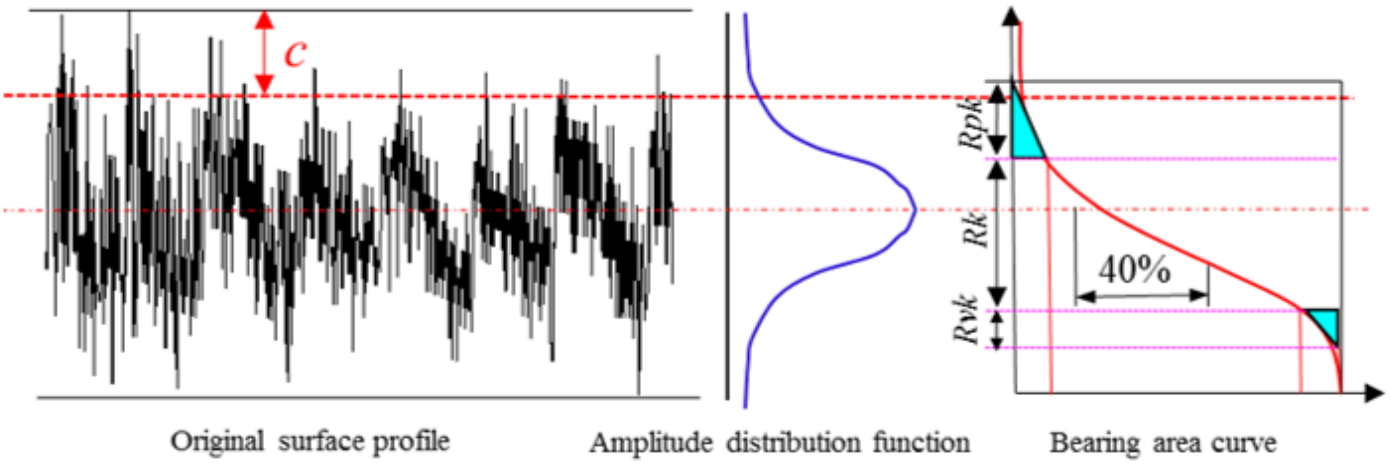

Figure 4

The 2D surface profile and corresponding ADF and BAC

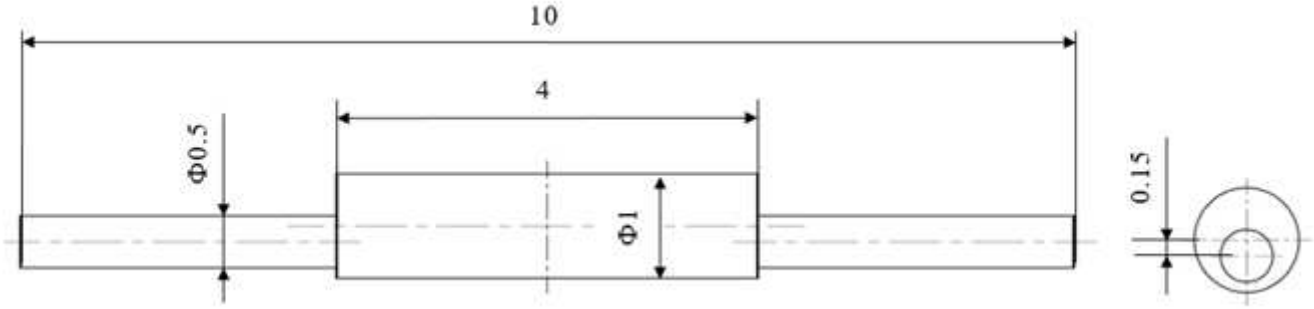

Figure 5

The size information of the micro eccentric shaft

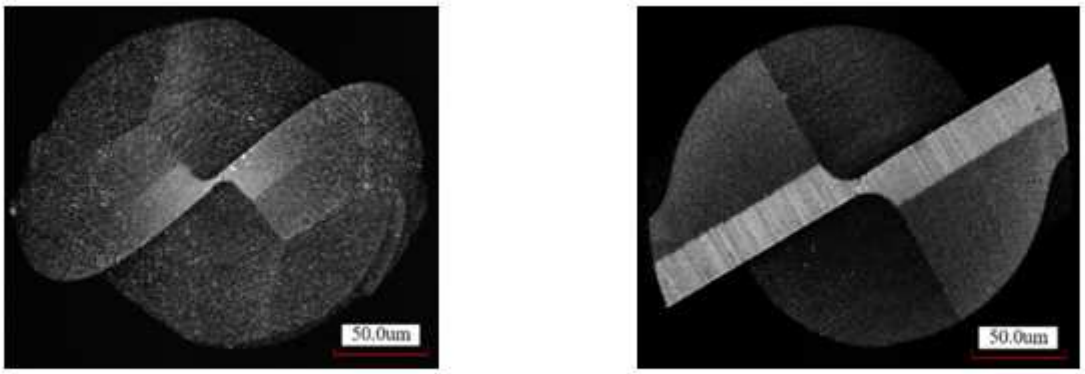

Figure 6

The micro milling cutter

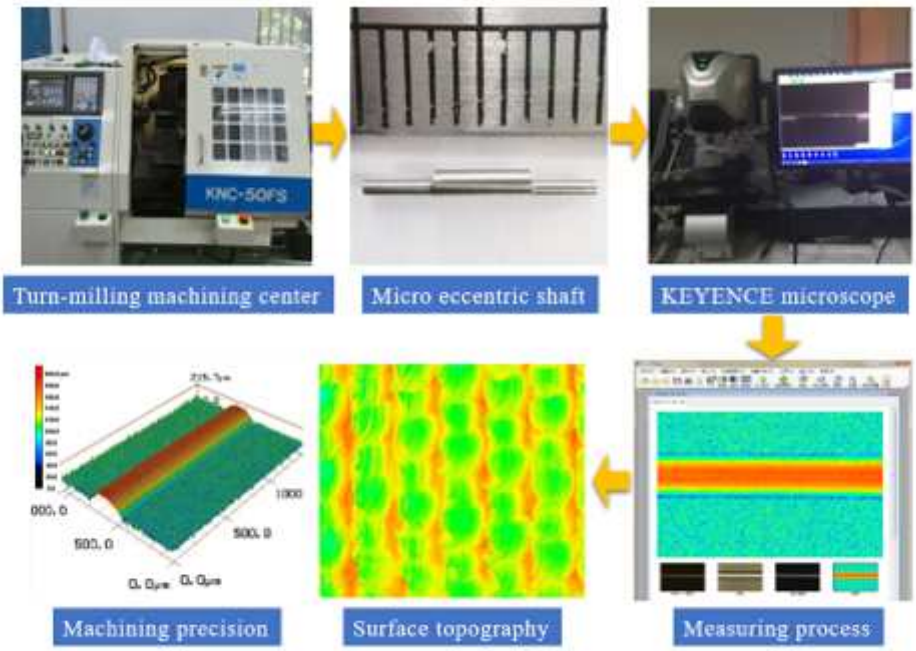

Figure 7

Turn-milling and measuring process

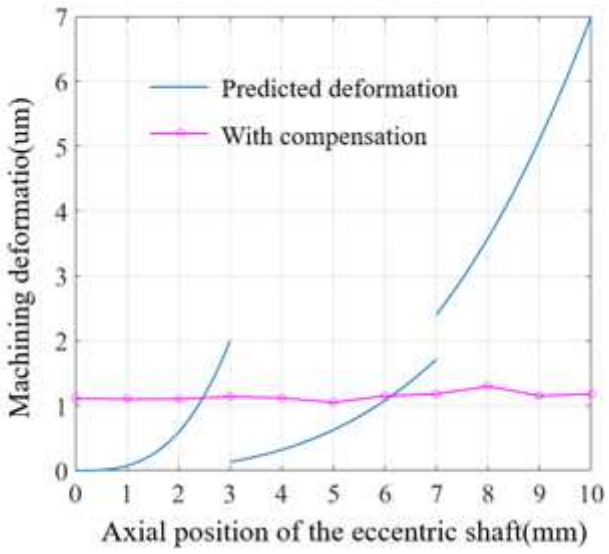

Figure 8

The machining deformation of micro eccentric shaft

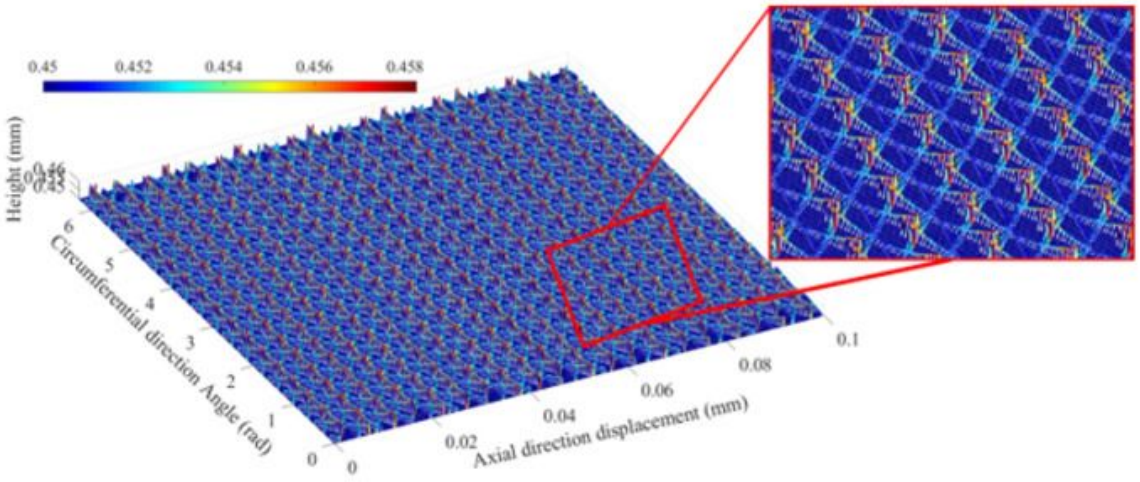

(a) The simulation result of surface texture of flat end milling cutter

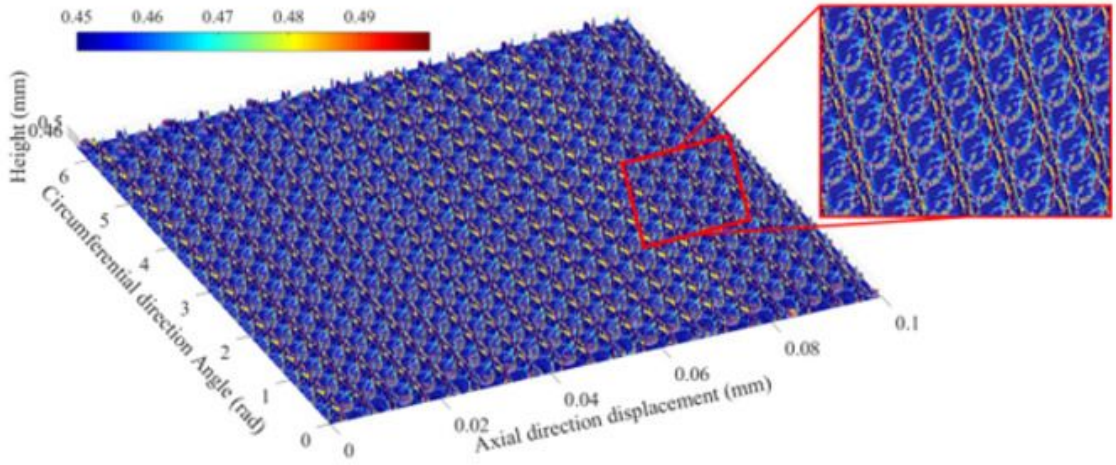

(b) The simulation result of surface texture of ball end milling cutter

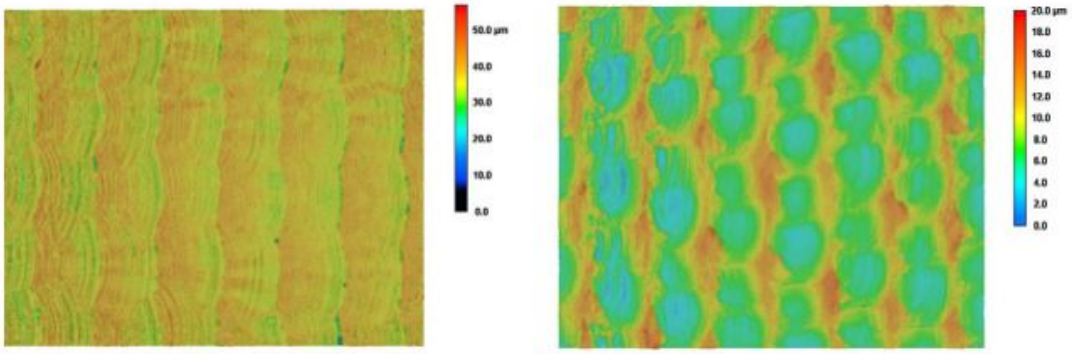

(c) Experimental result of flat end milling cutter

(d) Experimental result of ball end milling cutter

Figure 9

Surface texture profiles with different cutting tools.

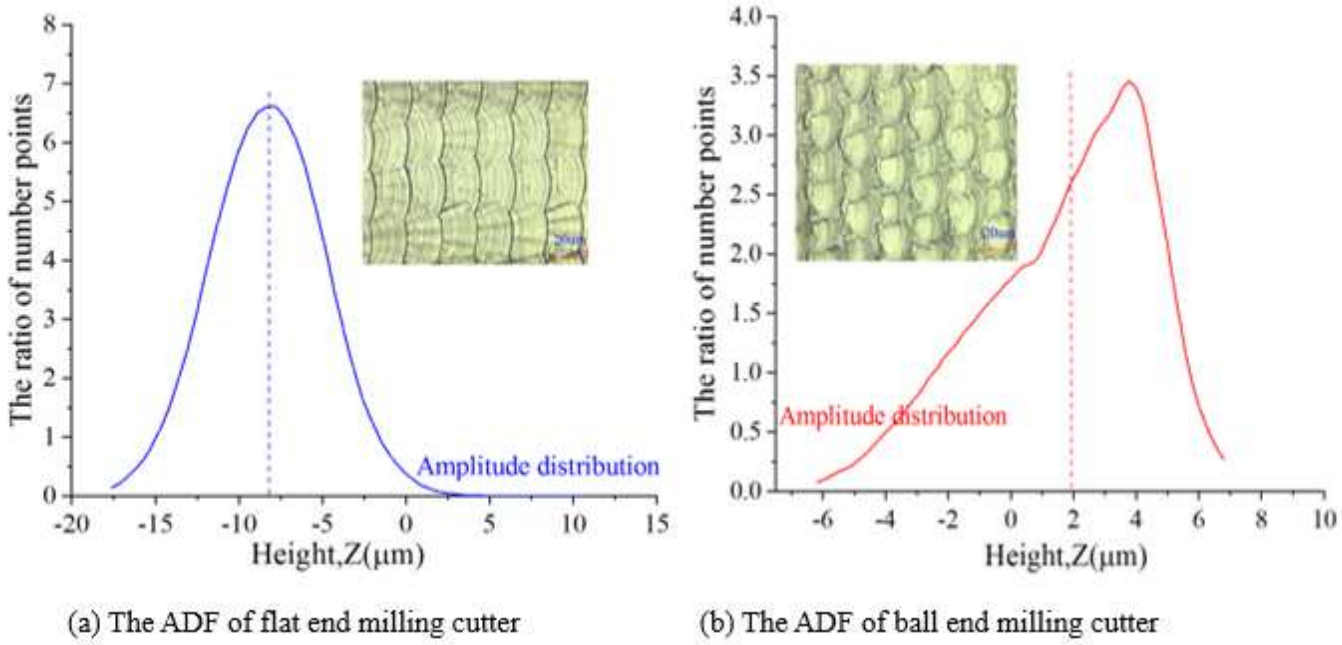

Figure 10

ADFs under different cutting tools

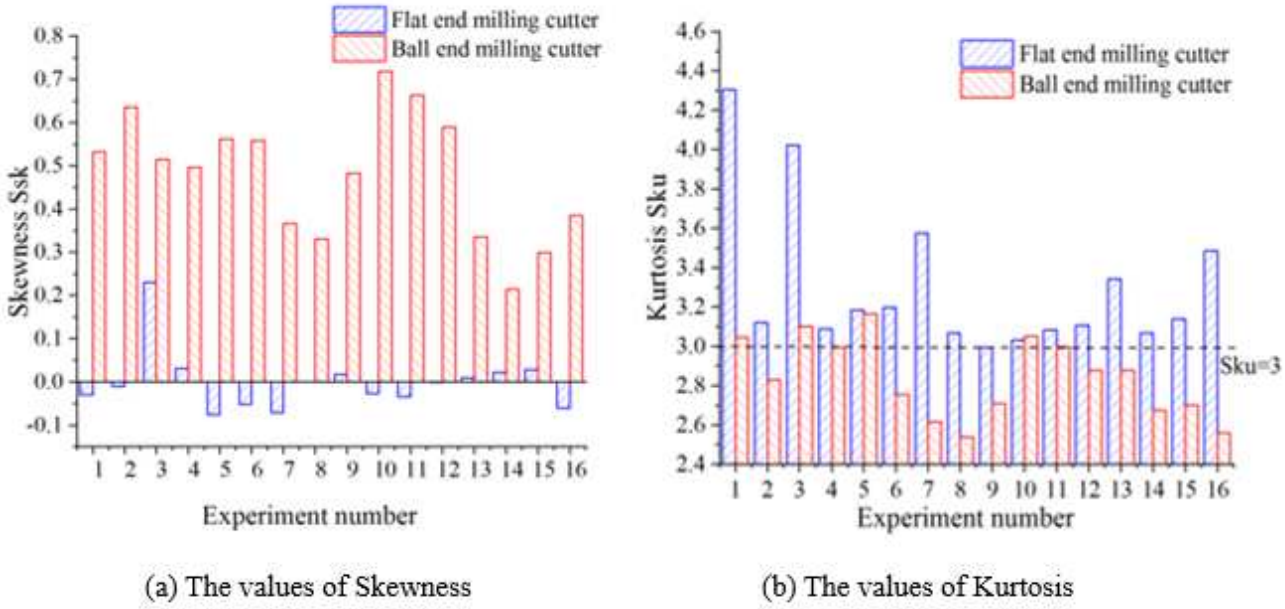

Figure 11

Statistical parameters of the machined surface

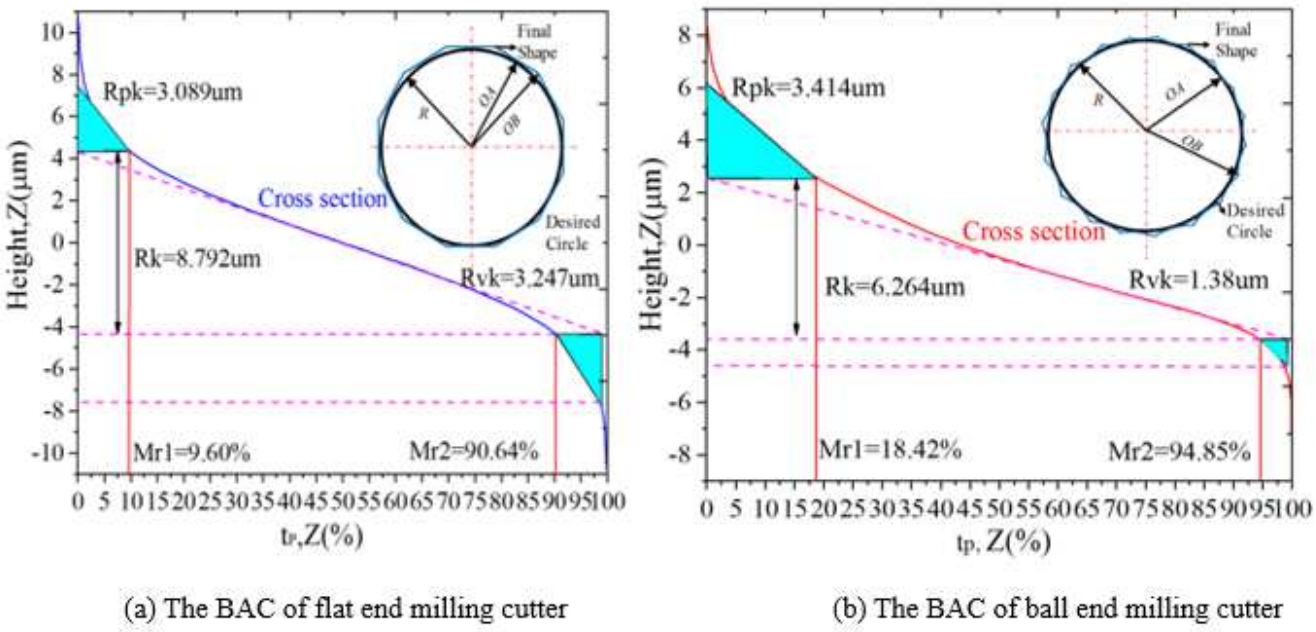

(a) The BAC of flat end milling cutter

(b) The BAC of ball end milling cutter

Figure 12

BAC under different cutting tools

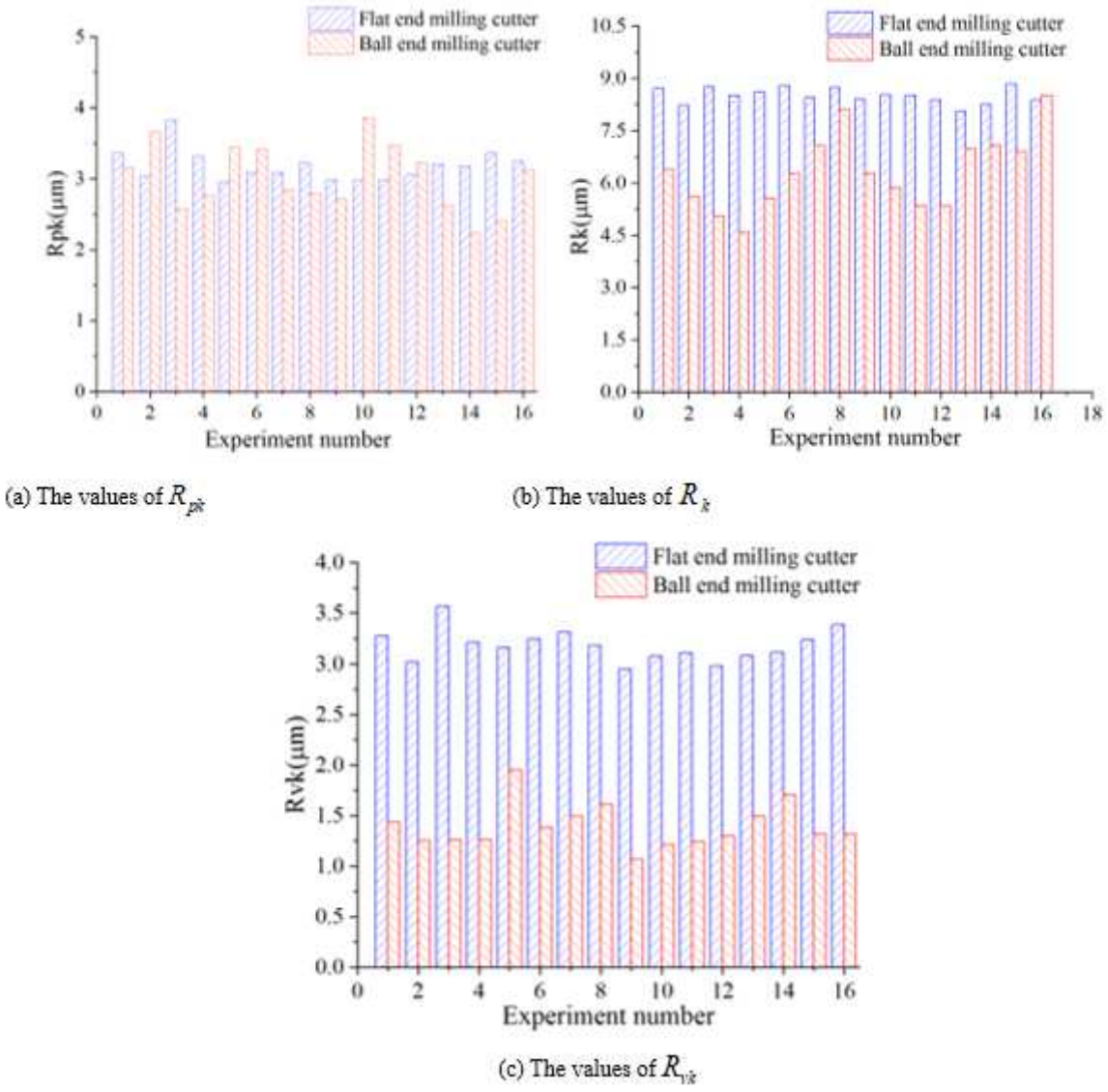

Figure 13

Functional statistical parameters under all cutting parameter combinations

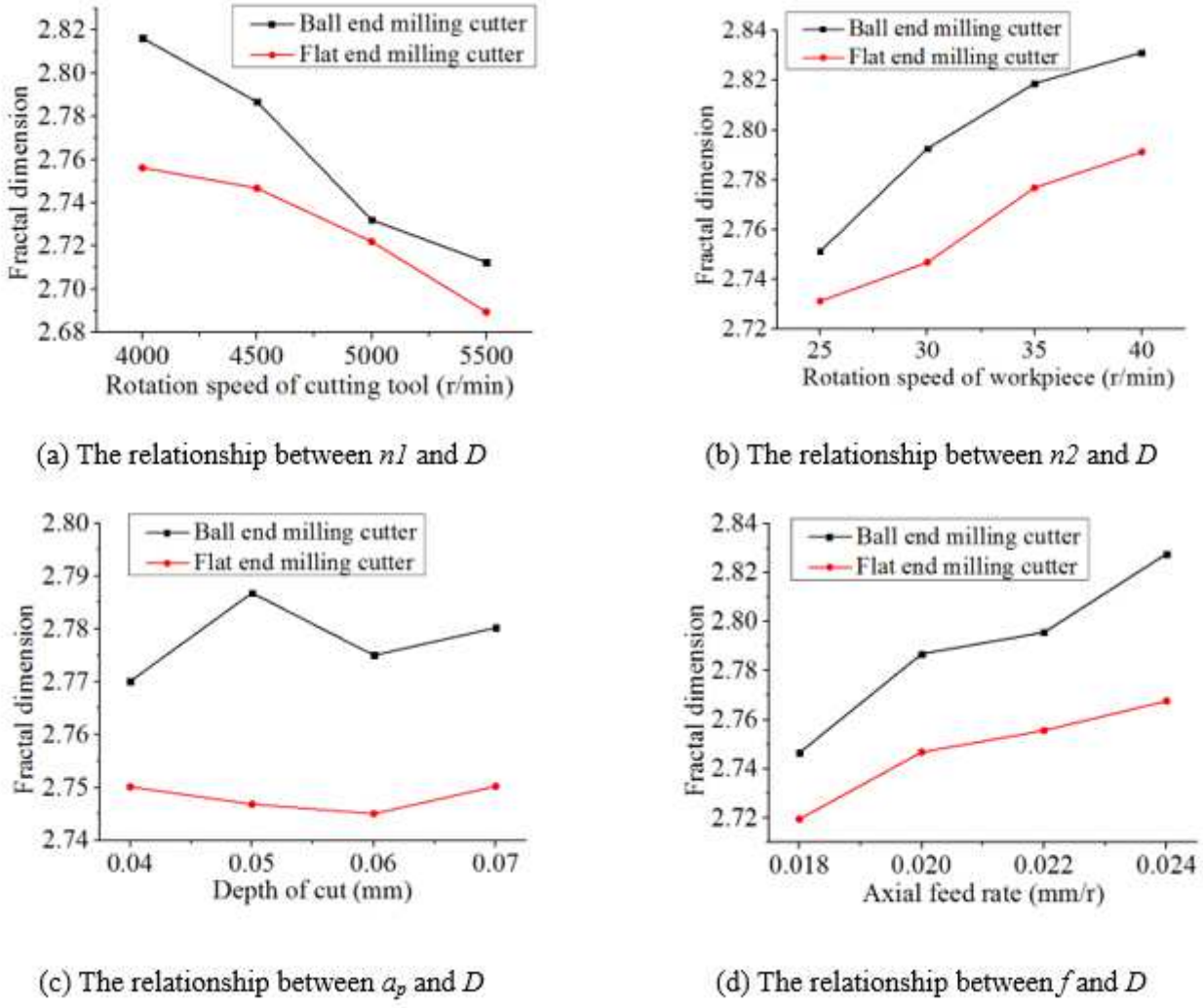

Figure 14

The relationship between cutting parameters and fractal dimension D

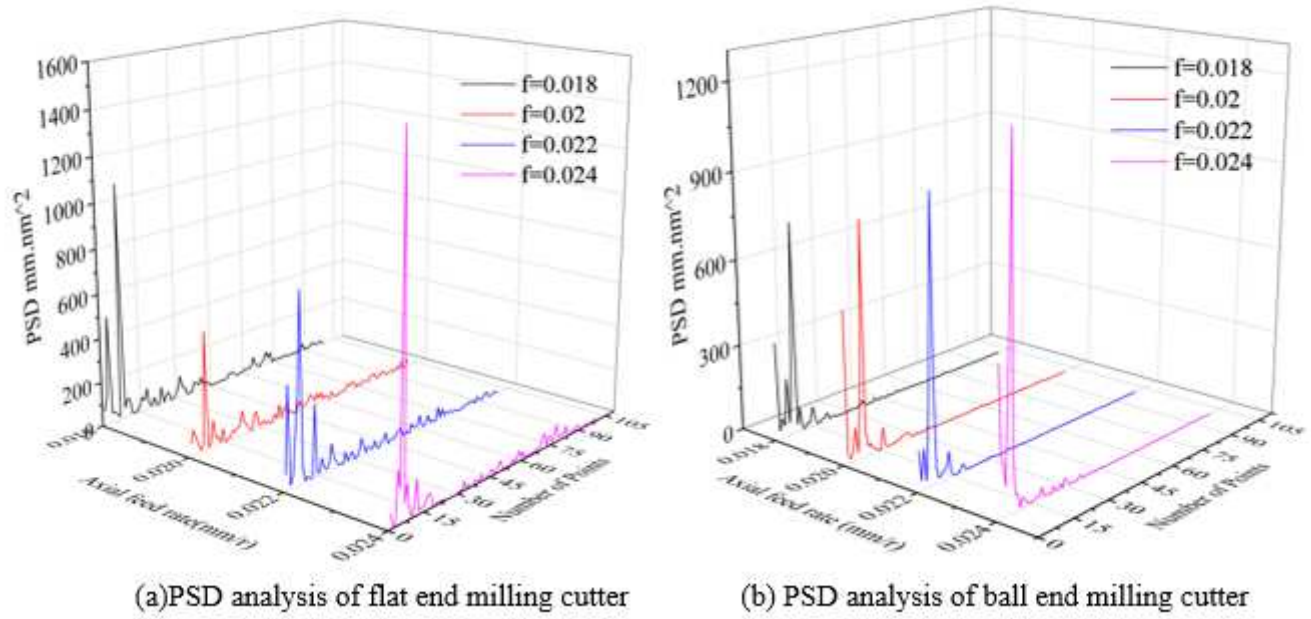

Figure 15

PSD analysis results under different cutting parameters

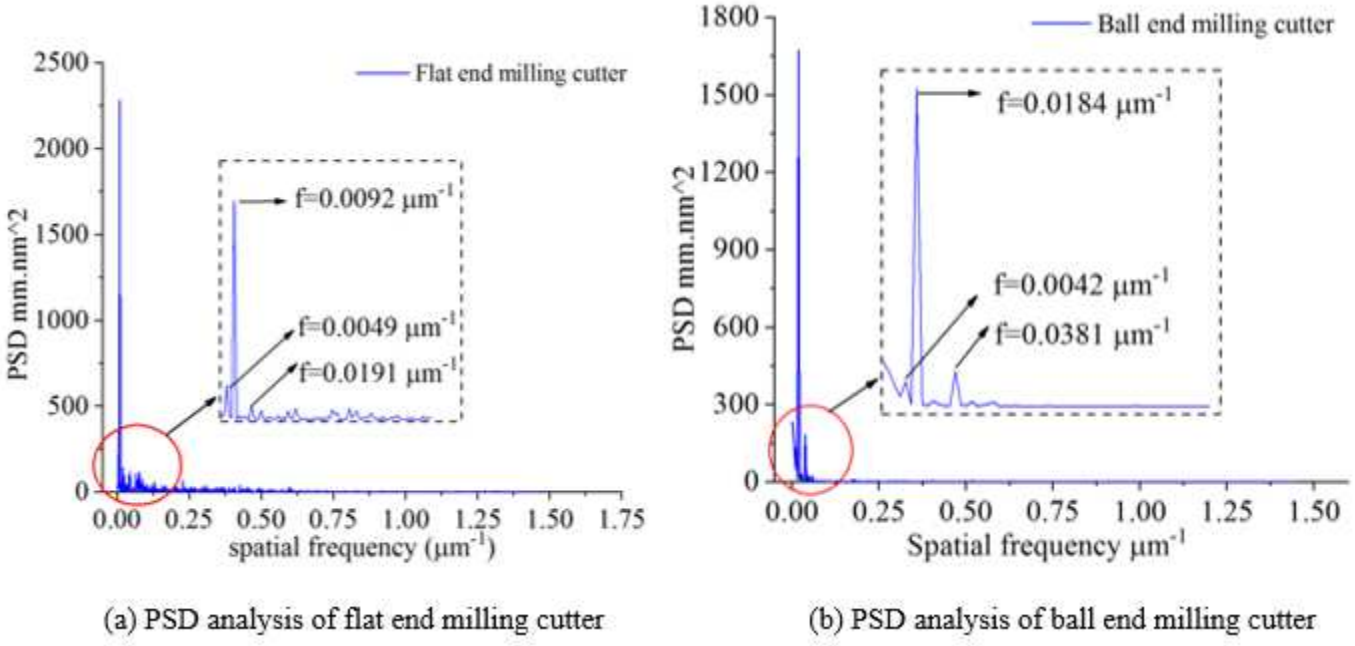

Figure 16

PSD analysis under different cutting tools

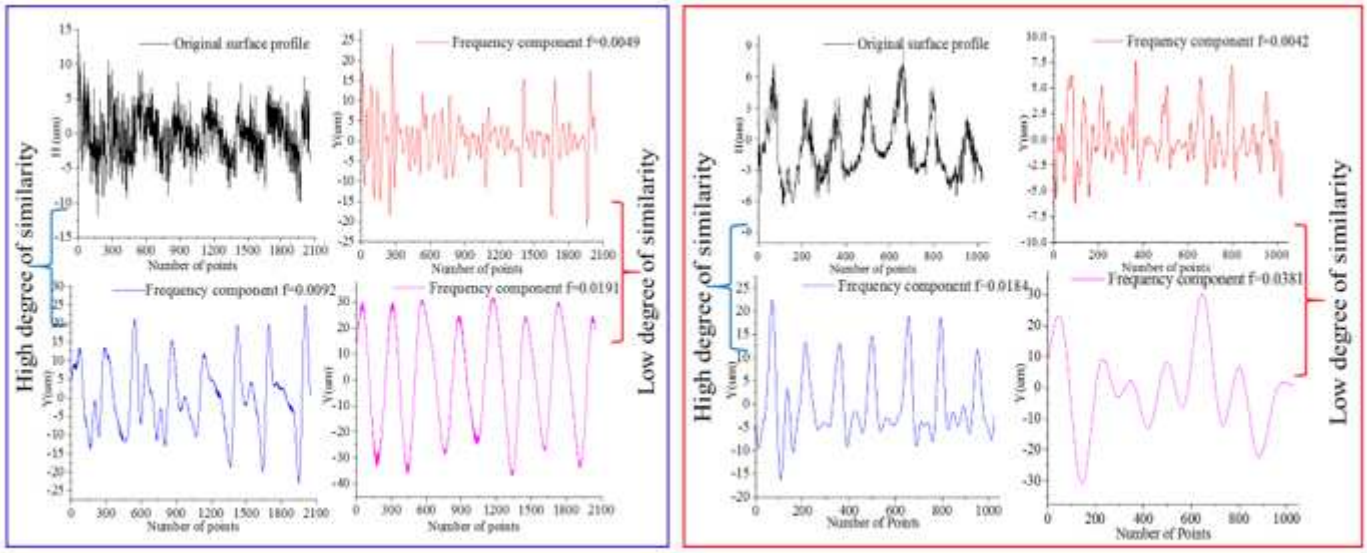

(a) CWT analysis of flat end milling cutter

(b) CWT analysis of ball end milling cutter

Figure 17